A polynomial based approach to extract the maxima of an antipodally symmetric spherical function and its application to extract fiber directions from the Orientation Distribution Function in Diffusion MRI *

Aurobrata Ghosh[1], Elias Tsigaridas[2], Maxime Descoteaux[3], Pierre Comon[4], Bernard Mourrain[2], and Rachid Deriche[1]

[1] Odyssee, INRIA Sophia Antipolis, France, Aurobrata.Ghosh@sophia.inria.fr,
[2] GALAAD, INRIA Sophia Antipolis, France,
[3] Neurospin, CEA Saclay, France,
[4] Laboratoire I3S, CNRS and the University of Nice, Sophia Antipolis, France.

Abstract. In this paper we extract the geometric characteristics from an antipodally symmetric spherical function (ASSF), which can be described equivalently in the spherical harmonic (SH) basis, in the symmetric tensor (ST) basis constrained to the sphere, and in the homogeneous polynomial (HP) basis constrained to the sphere. All three bases span the same vector space and are bijective when the rank of the SH series equals the order of the ST and equals the degree of the HP. We show, therefore, how it is possible to extract the maxima and minima of an ASSF by computing the stationary points of a constrained HP.
In Diffusion MRI, the Orientation Distribution Function (ODF), represents a state of the art reconstruction method whose maxima are aligned with the dominant fiber bundles. It is, therefore, important to be able to correctly estimate these maxima to detect the fiber directions. The ODF is an ASSF. To illustrate the potential of our method, we take up the example of the ODF, and extract its maxima to detect the fiber directions. Thanks to our method we are able to extract the maxima without limiting our search to a discrete set of values on the sphere, but by searching the maxima of a continuous function. Our method is also general, not dependent on the ODF, and the framework we present can be applied to any ASSF described in one of the three bases.

1 Introduction

In Diffusion MRI there exist numerous state of the art reconstruction algorithms which attempt to recover an integrated image by incorporating partial and directional information from diffusion weighted (DW) signals. The reconstructed

* Partially supported by the contracts ANR-06-BLAN-0074 "Decotes" and INRIA-ARC Diffusion-MRI.

and integrated image is often represented as values on a sphere at every voxel. The geometric characteristics of these antipodally symmetric spherical functions (ASSF) provide a sub-voxel resolution superior to the raw DW-MR images.

There are numerous aquisition schemes, and many reconstruction algorithms, that result in a number of distinct ASSFs, which represent different physical phenomena. For example there exist Diffusion Tensor Imaging (DTI) [1] which represents the Apparent Diffusion Coefficient (ADC), Generalized DTI (GDTI) [2–4] which also represents the ADC, Q-ball imaging (QBI) [5, 6] which represents the Orientation Distribution Function (ODF), Spherical Deconvolution (SD) which represents the fiber Orientation Density (fOD), and Maximum Entropy Spherical Deconvolution (MESD) [7] which is a generalization of the Persistent Angular Structure (PAS) method, and which recovers the angular structure of the particle displacement probability density function; to enumerate a few methods.

For certain of these ASSFs, their geometric characteristics have direct physical consequences. For example the maxima of the ODF and the fOD correspond to the fiber bundle directions. It is, therefore, important to be able to correctly estimate the maxima of these ASSFs to detect fiber directions (see Fig-1).

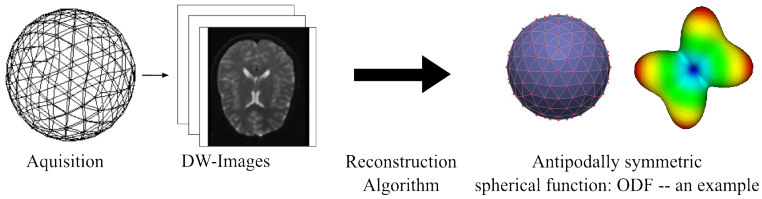

Fig. 1. An antipodally symmetric spherical function (ASSF) reconstructed from DWIs. The maxima of the ODF, for example, indicate fiber bundles. It is important to correctly estimate the maxima of these ASSFs.

It is common to analytically represent an ASSF in the Spherical Harmonic (SH) basis – analytical QBI for example, or in the Symmetric Tensor[5] (ST) basis constrained to the sphere – DTI or GDTI for example. These bases are bijective when the rank of the SH series equals the order of the symmetric tensor. The basis of Homogeneous Polynomials (HP) constrained to the sphere, is also bijective to the ST basis and spans the same vector space when the degree of the HP equals the order of the ST. It is, therefore, possible to represent an ASSF described in either the SH basis or the ST basis as a constrained HP.

In this paper, we take advantage of this constrained HP representation of an ASSF, to extract the maxima of the ASSF, by computing the stationary points of the constrained HP. We then rank the stationary points by their polynomial values to extract the maxima of the ASSF (see Fig-2).

[5] A symmetric tensor of any order requires that the coordinate array representating the tensor be invariant under all permutation of indices. It is often also referred to as a *supersymmetric* tensor.

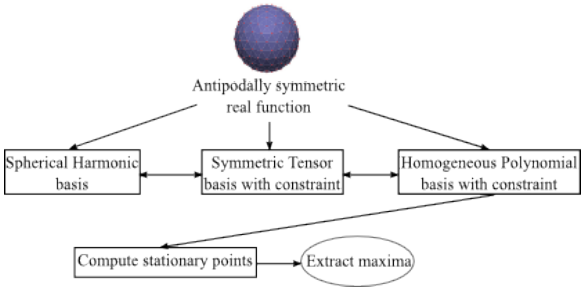

Fig. 2. An antipodally symmetric spherical function (ASSF) can be represented in three equivalent bases – spherical harmonics, symmetric tensor constrained to the sphere, or homogeneous polynomial (HP) constrained to the sphere. As a constrained HP it is possible to compute its stationary points to extract the maxima of the ASSF.

We illustrate our method on the ODF by computing its maxima, which correspond to fiber bundle directions. This method is, however, independent of the ODF, or of the ODF estimation process. It is, therefore, applicable to any ASSF that can be represented in either the SH, ST or HP basis. Also, since it is independent of the estimation process of the ASSF (ODF for example), this method, as we shall see, can be used to quantize the error of the estimation process of the ASSF. This can have important implications for evaluating the quality of the estimation process (ODF for example).

Another strength of our method, lies in the fact that it is not limited to searching for the maxima of the ASSF in a finite set of values on the sphere, but rather searches the maxima of a continuous function.

2 Methods

We begin the methods section by establishing the equivalence of the SH, ST and HP bases when describing an ASSF. First let us consider the ST and the HP bases, and then the HP and SH bases.

2.1 SH basis, constrained ST basis, constrained HP basis There is a useful connection between the space of STs and the space of HPs, e.g.[8, 9]. A symmetric tensor of dimension n and order d has a one-to-one correspondance with a homogeneous polynomial in n variables of total degree d. For example if we consider a 4-way array of dimension 3, then a tensor element $a_{ijk\ell}$, is associated to the monomial $a_{ijk\ell}x_ix_jx_kx_\ell$ and the whole tensor to the homogeneous polynomial $\sum_{i=1}^{3}\sum_{j=1}^{3}\sum_{k=1}^{3}\sum_{\ell=1}^{3} a_{ijk\ell}x_ix_jx_kx_\ell$. In other words, for an order d symmetric tensor of dimension n, an individual index i, j, $k, \ldots$, can take values from 1 to n, and the total number of indices qualifying a tensor element a (in the case of $a_{ijk\ell}$, it is four) has to be d. A similar construction exists for non-symmetric tensors and multi-homogeneous polynomials.

To illustrate this through an example, consider the $2 \times 2 \times 2$ tensor, i.e. order three symmetric tensor $\mathbf{A}$ of dimension two, with $a_{111} = 1$, $a_{121} = a_{211} = a_{112} = 2$, $a_{221} = a_{122} = a_{212} = 3$ and $a_{222} = 4$. The tensor consists of two 2×2 slices, i.e.

$$\mathbf{A}(:: 1) = \begin{bmatrix} 1 & 2 \\ 2 & 3 \end{bmatrix} \quad \text{and} \quad \mathbf{A}(:: 2) = \begin{bmatrix} 2 & 3 \\ 3 & 4 \end{bmatrix}.$$

The element a_{111} maps to the monomial x_1^3, the elements a_{121}, a_{211} and a_{112} map to the monomial $2x_1^2x_2$, the elements a_{221}, a_{122} and a_{212} map to the monomial $3x_1x_2^2$, and a_{222} maps to $4x_2^3$. Finally, $\mathbf{A}$ corresponds to the homogeneous polynomial $f = x_1^3 + 6x_1^2x_2 + 9x_1x_2^2 + 4x_2^3$.

Now let us consider the SH basis and the HP basis. Spherical functions are naturally decomposed and expressed in a SH basis because SHs form an orthonormal basis for complex functions on the sphere and have many properties that facilitate computation [10, 11]. The correspondence between coefficients of the real and symmetric SH series and the coefficients of the HP constrained to the sphere are derived here.

In [2, 12], it was proved that both even order SHs up to rank d and the HPs of degree d restricted to the sphere are bases for the same vector space. It is, therefore, possible to define a general linear transformation $\mathbf{M}$ between the two bases which shall be recomputed here by expressing the coefficients of the modified SH series c_j in terms of the coefficients of the homogeneous polynomial.

Let an ASSF S be decomposed in the modified SH basis such that [10, 11, 2, 12],

$$c_j = \int_\Omega S(\mathbf{g}(\theta, \phi))Y_j(\theta, \phi)d\Omega, \tag{1}$$

where $\mathbf{g}(\theta, \phi)$ is a normalized radial direction in spherical coordinates and Y_j is the jth coefficient of the real and symmetric SH basis [12].

Given a homogeneous polynomial P of degree d in three variables and constrained to the sphere

$$\mathrm{P}(\mathbf{x} = [x_1, x_2, x_3]^t) = \sum_{i_1=1}^{3} \sum_{i_2=1}^{3} \cdots \sum_{i_d=1}^{3} a_{i_1 i_2 \cdots i_d} x_{i_1} x_{i_2} \cdots x_{i_d}, \tag{2}$$

where $a_{i_1 i_2 \cdots i_d}$ are also the elements of the corresponding order d symmetric tensor $\mathbf{A}$ of dimension three, and $\mathbf{x}$ is of unit length to constrain P to the sphere; P can be rewritten in the form

$$\mathrm{P}(\mathbf{x}) = \sum_{k=1}^{N} \mu_k a_k \prod_{p=1}^{d} x_k(p), \tag{3}$$

where N are the number of independent elements of $\mathbf{A}$, a_k is the k^{th} independent element of $\mathbf{A}$, μ_k is its corresponding multiplicity, and $\prod_{p=1}^{d} x_k(p)$ is the corresponding monome (see[12]).

If P also describes the same ASSF S, then S in (1) can be replaced by (3) to obtain an expression in matrix form, where c_j is the jth element of the vector $\mathbf{C} = \mathbf{MA}$ and d is the number of elements in the SH basis:

$$c_j = \sum_{k=1}^{N} a_k \int_{\Omega} \mu_k \prod_{p=1}^{d} x_{k(p)}(\theta,\phi) Y_j(\theta,\phi) d\Omega \Longrightarrow \mathbf{C} = \mathbf{MA}\,, \text{ where} \tag{4}$$

$$\mathbf{M} = \begin{pmatrix} \mu_1 \int_{\Omega} \prod_{p=1}^{d} x_{1(p)}(\theta,\phi) Y_1(\theta,\phi) d\Omega & \dots & \mu_N \int_{\Omega} \prod_{p=1}^{d} x_{N(p)}(\theta,\phi) Y_1(\theta,\phi) d\Omega \\ \vdots & \ddots & \vdots \\ \mu_1 \int_{\Omega} \prod_{p=1}^{d} x_{1(p)}(\theta,\phi) Y_N(\theta,\phi) d\Omega & \dots & \mu_N \int_{\Omega} \prod_{p=1}^{d} x_{N(p)}(\theta,\phi) Y_N(\theta,\phi) d\Omega \end{pmatrix}. \tag{5}$$

It has been shown in [12] that the N x N square matrix $\mathbf{M}$ is a change-of-basis matrix, and is invertible. Therefore, given a vector $\mathbf{C}$ of SH coefficients, $\mathbf{M}^{-1}$ can be used to compute the coefficients of the constrained HP.

This establishes the bijectivity between the the SH basis, the constrained ST basis, and the constrained HP basis.

2.2 Constrained Polynomial maxima extraction Now that it is possible to express an ASSF in terms of a HP constrained to a sphere, the problem of determining the maxima of the ASSF reduces to computing the stationary points of the homogeneous polynomial P on the unit sphere. Once the stationary points are all computed, they can be sorted by their values in P to threshold and extract the maxima.

Therefore, to be more specific the following non-linear optimization problem has to be solved

$$\max_{\mathbf{x}} \mathrm{P}(\mathbf{x}) \text{ subject to } \|\mathbf{x}\|_2^2 - 1 = 0, \tag{6}$$

where $\mathbf{x} = (x_1, x_2, \dots, x_n)$ are the variables and P is of degree d, i.e. $\mathrm{P} \in \mathbb{R}[\mathbf{x}]_d$. In our case, d is even and $n = 3$.

The size of the problem (6) (degrees of the polynomials involved, number of solutions) is relatively small, and thus there is no need to rely on general algorithms for polynomial optimization subject to constraints, e.g. [13]. Instead, we use the method of Lagrange multipliers for our problem. The reader may also refer to Karush-Kuhn-Tucker conditions [14] that provide the necessary conditions for the solution to (6) to be optimal.

We consider the polynomial $F(\mathbf{x}, \lambda) = \mathrm{P}(\mathbf{x}) - \lambda\,(\|\mathbf{x}\|_2^2 - 1)$. Then, the solution(s) of (6) is (are) among the solutions of the system

$$\frac{\partial F}{\partial x_1} = \frac{\partial F}{\partial x_2} = \cdots = \frac{\partial F}{\partial x_n} = \|\mathbf{x}\|_2^2 - 1 = 0. \tag{7}$$

It is easy to see that the equations in (7) are linear in λ. Thus one can be solved for λ and substituted in the others. The derived system is equivalent to

the system obtained by requiring the vectors $\nabla \mathrm{P}$ and $\mathbf{x} = [x_1, x_2, \ldots, x_n]$, to be parallel. This yields the system

$$\begin{vmatrix} \frac{\partial \mathrm{P}}{\partial x_i} & x_i \\ \frac{\partial \mathrm{P}}{\partial x_j} & x_j \end{vmatrix} = 0 \text{ for } 1 \leq i < j \leq n \text{ and } \|\mathbf{x}\|_2^2 - 1 = 0.$$

This system describes the values $\mathbf{x}$ that maximize P on the unit sphere but also the other points where P has local extrema. For $n = 3$ variables and P a polynomial of degree $d = 4$, we obtain 3 equations of degree 4 and one of degree 2. One of them (of degree 4) being redundant, by Bezout's theorem this system has at most $4 \times 4 \times 2 = 32$ solutions. If $\mathbf{x}$ is a solution, them $-\mathbf{x}$ is also a solution. Thus the system defines at most 16 directions for the local extrema of P.

We choose to solve the corresponding systems combining two of the state of the art algorithms in polynomial system solving, i.e. subdivision methods and generalized normal forms algorithms. We solve the system using both methods and keep the best solutions by evaluating them in the polynomial system. The main virtue of both the algorithms is that they rely on algebraic techniques and thus unlike numerical iterative methods for polynomial system solving, they are neither slow, and nor do they diverge when dealing with ill conditioned systems.

Subdivision methods [15] approximate only the real solutions. Initialy, they consider a hyper-box where all the (real) solutions of the system are searched (here one can take the box $[-1, 1]^3$ which contains the unit sphere) and they subdivide it until a specified precision is reached, excluding boxes which do not contain roots. Preconditionning techniques are exploited to speed up the root approximation process. Bounding techniques are used to handle properly polynomials with approximate coefficients.

The other family of algorithms that can also be applied to polynomials with approximate coefficients is based on generalized normal form computations [16], which extend classical Gröbner basis methods [17]. Unlike Gröbner basis, this algorithm is numerical stable and thus suitable for solving polynomial systems with approximate coefficients. The method exploits the multiplicative structure of the quotient algebra of the polynomial ring by the (zero dimensional) ideal generated by a system of polynomial equations. Eventually, the resolution of the polynomial system is transformed into a generalized eigenvalue and eigenvector problem [18]. In practice, all the complex roots are computed within some tolerance, and those which are (almost) real are kept.

2.3 Analytical spherical harmonic estimation of the ODF Having established the theoretical framework of our method, we would like to illustrate it on a concrete example. We pick for that purpose the ODF computed analytically in the SH basis from QBI. The ODF is an ASSF. We, therefore, present for completeness, the analytical ODF estimation from High Angular Resolution Diffusion Imaging (HARDI) aquisitions. Our approach is, however, independent of the ODF or the ODF estimation process, and can be applied to any ASSF expressed in one of the SH, the ST or the HP bases.

The diffusion ODF is defined as the angular portion of the averaged diffusion PDF. It can be obtained from diffusion spectrum imaging (DSI) or from QBI. [5] showed that it was possible to reconstruct the diffusion ODF directly from raw HARDI measurements on a single sphere by the Funk-Radon transform (FRT). The ODF is intuitive because it has its maximum(a) aligned with the underlying population of fiber(s). [6, 19] proposed a simple analytical spherical harmonic (SH) reconstruction of the ODF. The FRT integral can be evaluated analytically which leads to a linear, robust and computationnally fast ODF reconstruction.

Letting Y_d^m denote the SH of rank d and degree m ($m = -d, ..., d$) in the standard basis and Y_j ($j(d, m) = (d^2 + d + 2)/2 + m$) be the SH in the modified real and symmetric basis [12, 6], the analytical ODF solution is

$$\Psi(\theta, \phi) = \sum_{j=1}^{N} \underbrace{2\pi P_{d(j)}(0) c_j}_{f_j} Y_j(\theta, \phi), \tag{8}$$

where $N = (d + 1)(d + 2)/2$, c_j are the SH coefficients describing the input HARDI signal [12], f_j are the SH coefficients describing the ODF Ψ, d_j is the rank associated with j^{th} SH basis element (for $j = \{1, 2, 3, 4, 5, 6, 7, ...\}$, $d_j = \{0, 2, 2, 2, 2, 2, 4, ...\}$) and P_{d_j} a Legendre polynomial.

3 Experiments

For our initial experiments, we test our method for a SH basis of rank-4, or equivalently a ST basis of order-4, or equivalently a HP basis of degree-4.

We test on synthetic data with known ground truth maxima directions. We perform two types of tests along similar lines. We consider an ASSF to be a set of scalar values defined on a sphere. In the first type of tests we generate a spherical function with four maxima (antipodally symmetric, therefore, we can consider the maxima to be along two distinct directions), to test our approach on a purely mathematical framework. We generate the spherical function by first randomly choosing the two maxima-directions separated by a pre-defined angle. Along these directions (and their opposite directions) we then set the function to have value 1, and everywhere else on the sphere to have value 0. Essentially we generate a spherical dirac function. We then fit a rank-4 SH function to this spherical data, for our maxima extraction tests. We call this the dirac test (section-3.1).

In the second type of tests, we use the multi-tensor model [12], to synthetically generate DW signals with fiber crossings. We simulate one and two fiber voxels with known ground truth directions. In the case of two fiber voxels, the two fibers have equal volume fractions are are separated by 90^o. The diffusion tensor profile used for a fiber has diag($\mathbf{D}$) = [1390,355,355]x10^{-6} mm^2/s, FA = 0.7 which corresponds to our real dataset diffusion profile. This synthetic data generation is relatively standard and has the advantage of producing known ground truth ADC and ODF profiles as well as ground truth fiber orientations. We add

no noise to the signal. We then estimate the analytical ODF in the SH basis with rank-4 from this signal, on which we perform the maxima extraction tests. We call this the ODF test (section-3.2).

Both tests, essentially involve three steps, which can be summarized as:

1. A set of ground truth directions $\{d_i\}$ are used to generate either a set of values on the sphere (section-3.1) or DW signals (section-3.2) such that the maxima of the set of values on the sphere or the ODF estimated from the DW signals respectively, have their maxima alligned with $\{d_i\}$.
2. In section-3.1 we estimate a rank-4 SH series to best fit the set of values on the sphere. In section-3.2 we estimate an ODF of rank-4 from the DW signals.
3. We then convert the SH coefficients to the HP basis (or the equivalent ST basis) and formulate the constrained polynomial problem, which we call $\mathcal{F}$. We compute its stationary points $\{R_j\}$, and sort them by their polynomial value, and then threshold the list to retrieve a set of computed maxima $\{d_k^{'}\}$.

We then proceed to compare $\{d_k^{'}\}$ to $\{d_i\}$. This is only possible when $k = i$. When the two sets are comparable, we pair the computed directions with the ground truth directions such that their difference is minimized. Then we first compute the angle between d_i and $d_i^{'}$ in degrees which we denote as $ang(d_i, d_i^{'})^o$. If this angle is non zero, we proceed to quantize the errors in steps 1, 2 and 3. Since, $\{d_i^{'}\}$ are the stationary points of $\mathcal{F}$, the value of $||\nabla\mathcal{F}(d_i^{'})||$ indicates the amount of error in step 3. Computing $||\nabla\mathcal{F}(d_i)||$ on the other hand indicates the amount of error in steps 1 and 2. In both the dirac tests and the ODF tests the error in step 1 can be considered to be nominal, since in the dirac tests the spherical function is analytically generated, and in the ODF tests we don't use any noise while generating the DW signals. So essentially $||\nabla\mathcal{F}(d_i)||$ is a measure of the error in step 2, which for the dirac tests is a truncated SH fit, and for the ODF tests is a truncated ODF estimation.

3.1 Dirac test In these tests we have four antipodally symmetric maxima, or two distinct maxima-directions (the two other are the opposites of these), separated by a pre-decided angle. We test our method for separation angles of 65^o and of 90^o. We construct one hundred test cases for each separation angle,

	$ang(d, d^{'})^o$		$\|\|\nabla\mathcal{F}(d^{'})\|\|$		$\|\|\nabla\mathcal{F}(d)\|\|$	
	m	v	m	v	m	v
65^o	0.281947	0.165978	4.70385e-11	2.91655e-21	5.00318e-05	3.28434e-10
90^o	0.0308949	0.0242211	4.00631e-11	2.82319e-21	1.09740e-05	1.55176e-11

Table 1. (m=mean, v=variance). The correct number of maxima were extracted. $||\nabla\mathcal{F}(d^{'})||$ gives a measure of the error in step 3, and $||\nabla\mathcal{F}(d)||$ gives a measure of the error in step 2. The error in step 3 is orders of magnitude smaller than the error in step 2. Our approach can be used to quantify the error in step 2 due to the truncation of SH series.

but randomly chosen maxima-directions, to compute the maxima directions and to compare the errors in steps 2 and 3. Since two maxima are extracted, for all the errors computed, such as $ang(d_i, d_i^{'})^o$, $||\nabla\mathcal{F}(d_i)||$, and $||\nabla\mathcal{F}(d_i^{'})||$ we keep the maximum of the two errors in each test (and remove the index i). The results are presented in Table-1.

In each of these tests we extract the correct number of maxima. We, however, notice that for a rank-4 SH estimation of the dirac spherical function, if we decrease the separation angle from 65^o, then the maxima were not prominently distinct any more, and we did come across cases when the number of estimated directions didn't match the number of ground truth directions. We suspect, therefore, that our approach can be also used to determine the angular resolution of a truncated SH series, depending upon the truncation length.

We also realise that the error in step 3: $||\nabla\mathcal{F}(d^{'})||$, is orders of magnitude smaller than the error in step 2: $||\nabla\mathcal{F}(d)||$. Again our approach can be useful in determining the goodness of fit of a truncated SH series to a set of scalars defined on a sphere.

3.2 ODF test In these tests we used the multi-tensor model [12] to generate DW signals, from where we estimate the ODF in the SH basis with rank-4.

We again construct one hundred test cases for both the one fiber and the two fiber simulations, and the ground truth directions are chosen randomly. The results are summarized in Table-2. Again in each of the tests we extract the correct number of maxima. We notice that the mean error in step 2 of the ODF tests: $||\nabla\mathcal{F}(d)||$ (Table-2), i.e. the ODF estimation in the truncated (rank-4) SH basis, entails an error that is orders of magnitude larger than the mean error in step 2 of the dirac tests: $||\nabla\mathcal{F}(d)||$ (Table-1). This can be explained by the fact that the ODF estimation is a much more complex process than a simple rank-4 SH fit. The error in the ODF estimation step is of course much larger than the error in step 3: $||\nabla\mathcal{F}(d^{'})||$ (Table-2), where we compute the maxima using the homogeneous polynomial representation. A graphical illustration of our approach from this test can be seen in Fig-3a.

We also tested our method on real data[20] and successfully extracted maxima from ODFs with various fiber configurations. We tested in a region of interest (ROI) of a coronal slice, where complex fiber structures are known to exist in

	$ang(d, d^{'})^o$		$\|\|\nabla\mathcal{F}(d^{'})\|\|$		$\|\|\nabla\mathcal{F}(d)\|\|$	
	m	v	m	v	m	v
1-Fib	0.0104625	4.22152e-05	2.07053e-11	1.49751e-21	0.000490269	9.16956e-08
2-Fib$_{90^o}$	0.0254106	3.85231e-05	5.5777e-11	1.7602e-21	0.0036013	2.4827e-06

Table 2. (m=mean, v=variance). The correct number of maxima were extracted from the ODF estimation. $||\nabla\mathcal{F}(d^{'})||$ gives a measure of the error in step 3, and $||\nabla\mathcal{F}(d)||$ gives a measure of the error in step 2 – the ODF estimation. The error in step 3 is orders of magnitude smaller than the error in step 2. Our approach can be used to quantify the error in the ODF estimation due to the truncation of SH series.

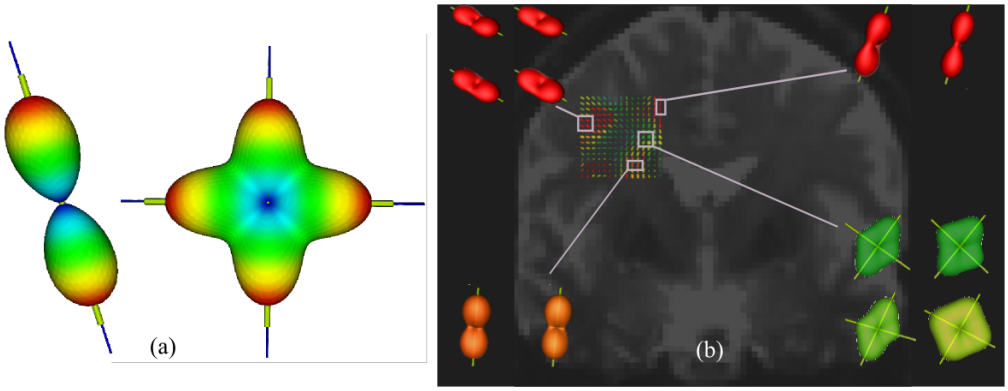

Fig. 3. Our approach applied to extract the maxima of an ODF in the SH basis with rank-4. **a)** We test on synthetic data, the dark blue lines are the ground truth directions. In the more prominent green are the computed directions. **b)** We test on a coronal slice of a real dataset within a region with complex fiber crossings. We see highlighted the fibers extracted by our method. We see that our approach can successfully extract the maxima of the ODF which are the fiber directions.

the white matter. The ROI contained fiber bundles from the cortico-spinal tract, superior longitudinal fibers (traversing the plane) and the corpus callosum (in the plane). The visual results can be viewed in Fig-3b.

Finally on the real dataset we compared our method against a discrete approach[6] which searches for the maxima on the discretized mesh of the ODF. For the discrete approach we used an icosahedron scheme on the sphere with tesselations of order 2, 3, 4, 5, 6 with 21, 81, 321, 1281, 5121 mesh-points respectively on a hemisphere. For the discrete method on each of these meshes and our approach, after extracting the maxima, we computed the error $||\nabla \mathcal{F}(d)||$ for each voxel and from there the mean and the variance. Figure-4 compares the mean error and the variance of the discrete approach on increasingly refined meshes to those of our method.

4 Discussion & Conclusion

We took advantage of the fact that an ASSF can be equivalently represented in any of three bijective bases – the SH basis, the ST basis constrained to the sphere, and the HP basis constrained to the sphere. This permitted us to extract the geometric characteristics, i.e. the maxima of an ASSF by computing the stationary points of a constrained homogeneous polynomial problem.

We tested this approach on synthetic tests, first on a purely mathematically generated dirac spherical function, and then on the ODF computed analytically in the SH basis. The ODF is a state-of-the-art reconstruction algorithm in diffusion MRI, who's maxima are aligned with the underlying dominant fiber bundles. Therefore, it is of utmost importance to be able to extract these maxima cor-

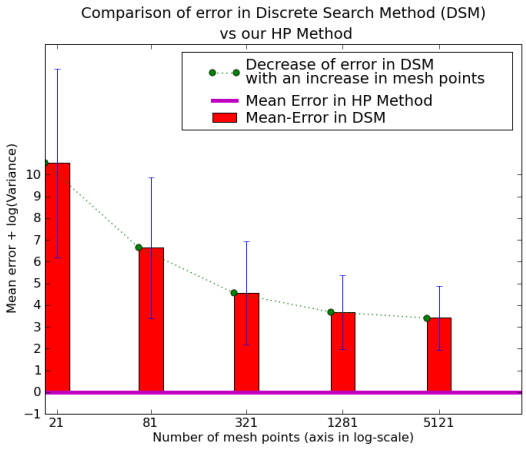

Fig. 4. Mean error ($||\nabla \mathcal{F}(d)||$: red bar) with ln of the variance (blue vertical intervals) of the discrete search method (DSM) plotted as a function of the mesh resolution, compared against our homogeneous polynomial (HP) method on a real dataset.

rectly. We took the ODF as an example, to concretely illustrate our method. But our method is independent of the ODF or of the ODF estimation process. It can be applied to any ASSF that can be written in either the SH basis, or the ST basis or the HP basis.

Our method has also the added strength of searching for the maxima of a continuous function, and is, therefore, not limited to searching for the maxima of an ASSF in a finite set of values on the sphere.

We tested our method with a rank-4 SH series, or equivalently order-4 ST, or equivalently a degree-4 HP. In the future we plan to test for greater values of rank/order/degree.

We also discovered that, using our polynomial approach, it was possible to quantify the error in the ODF estimation process that takes place due to the truncation of the SH basis to a finite rank. This interesting point could be further developed too.

References

1. Basser, P., Mattiello, J., LeBihan, D.: Estimation of the effective self-diffusion tensor from the NMR spin echo. Journal of Magnetic Resonance **B**(103) (1994) 247–254
2. Ozarslan, E., Mareci, T.: Generalized diffusion tensor imaging and analytical relationships between diffusion tensor imaging and high angular resolution imaging. Magnetic Resonance in Medicine **50** (2003) 955–965
3. Liu, C., Bammer, R., Acar, B., Moseley, M.E.: Characterizing non-gaussian diffusion by using generalized diffusion tensors. Magnetic Resonance in Medicine **51** (2004) 924–937

4. Barmpoutis, A., Jian, B., Vemuri, B.C.: Symmetric positive 4th order tensors & their estimation from diffusion weighted MRI. In: Information Processing in Medical Imaging (IPMI 2007). (2007)
5. Tuch, D.: Q-ball imaging. Magnetic Resonance in Medicine **52**(6) (2004) 1358–1372
6. Descoteaux, M., Angelino, E., Fitzgibbons, S., Deriche, R.: Regularized, fast, and robust analytical q-ball imaging. Magnetic Resonance in Medicine **58** (2007) 497–510
7. Alexander, D.C.: Maximum entropy spherical deconvolution for diffusion mri. In: Image Processing in Medical Imaging. (2005) 76–87
8. Comon, P., Mourrain, B., Lim, L., Golub, G.: Genericity and rank deficiency of high order symmetric tensors. Proc. IEEE Int. Conference on Acoustics, Speech, and Signal Processing (ICASSP) **31** (2006) 125–128
9. Comon, P.: Tensor decompositions. In McWhirter, J.G., Proudler, I.K., eds.: Mathematics in Signal Processing V. Clarendon Press, Oxford, UK (2002) 1–24
10. Frank, L.: Characterization of anisotropy in high angular resolution diffusion-weighted MRI. Magnetic Resonance in Medicine **47**(6) (2002) 1083–1099
11. Alexander, D., Barker, G., Arridge, S.: Detection and modeling of non-gaussian apparent diffusion coefficient profiles in human brain data. Magnetic Resonance in Medicine **48**(2) (2002) 331–340
12. Descoteaux, M., Angelino, E., Fitzgibbons, S., Deriche, R.: Apparent diffusion coefficients from high angular resolution diffusion imaging: Estimation and applications. Magnetic Resonance in Medicine **56** (2006) 395–410
13. Lasserre, J.: Global optimization with polynomials and the problem of moments. SIAM Journal on Optimization **11** (2001) 796–817
14. Karush, W.: Minima of functions of several variables with inequalities as side constraints. Master's thesis, Dept. of Mathematics, Univ. of Chicago, Chicago, Illinois (1939)
15. Mourrain, B., Pavone, J.P.: Subdivision methods for solving polynomial equations. Technical Report RR-5658, INRIA Sophia-Antipolis (2005)
16. Mourrain, B., Trébuchet, P.: Generalised normal forms and polynomial system solving. In Kauers, M., ed.: Proc. Intern. Symp. on Symbolic and Algebraic Computation, New-York, ACM Press. (2005) 253–260
17. Cox, D., Little, J., O'Shea, D.: Ideals, Varieties, and Algorithms: An Introduction to Computational Algebraic Geometry and Commutative Algebra. Undergraduate Texts in Mathematics. Springer Verlag, New York (1992)
18. Elkadi, M., Mourrain, B.: Introduction à la résolution des systèmes d'équations algébriques. Volume 59 of Mathématiques et Applications. Springer-Verlag (2007)
19. Hess, C., Mukherjee, P., Han, E., Xu, D., Vigneron, D.: Q-ball reconstruction of multimodal fiber orientations using the spherical harmonic basis. Magnetic Resonance in Medicine **56** (2006) 104–117
20. Anwander, A., Tittgemeyer, M., von Cramon, D.Y., Friederici, A.D., Knosche, T.R.: Connectivity-based parcellation of broca's area. Cerebral Cortex **17**(4) (2007) 816–825